

Polyelectrolyte adsorption onto like-charged surfaces mediated by trivalent counterions: A Monte Carlo simulation study

Germán Luque-Caballero, Alberto Martín-Molina, and Manuel Quesada-Pérez

Citation: *The Journal of Chemical Physics* **140**, 174701 (2014);

View online: <https://doi.org/10.1063/1.4872263>

View Table of Contents: <http://aip.scitation.org/toc/jcp/140/17>

Published by the [American Institute of Physics](#)

Articles you may be interested in

[Limiting Laws and Counterion Condensation in Polyelectrolyte Solutions I. Colligative Properties](#)

The Journal of Chemical Physics **51**, 924 (2003); 10.1063/1.1672157

[Charge renormalization, osmotic pressure, and bulk modulus of colloidal crystals: Theory](#)

The Journal of Chemical Physics **80**, 5776 (1998); 10.1063/1.446600

[Perspective: Coulomb fluids—Weak coupling, strong coupling, in between and beyond](#)

The Journal of Chemical Physics **139**, 150901 (2013); 10.1063/1.4824681

[Electrostatic origins of polyelectrolyte adsorption: Theory and Monte Carlo simulations](#)

The Journal of Chemical Physics **133**, 044906 (2010); 10.1063/1.3463426

[Polyelectrolyte adsorption on heterogeneously charged surfaces](#)

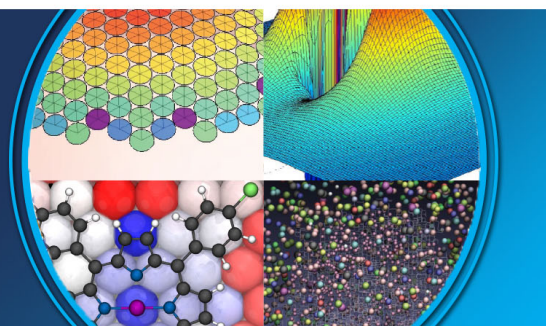
The Journal of Chemical Physics **112**, 8723 (2000); 10.1063/1.481474

[Adsorption of polyelectrolytes onto oppositely charged cylindrical macroions](#)

The Journal of Chemical Physics **138**, 244909 (2013); 10.1063/1.4811842

AIP | The Journal of
Chemical Physics

PERSPECTIVES



Polyelectrolyte adsorption onto like-charged surfaces mediated by trivalent counterions: A Monte Carlo simulation study

Germán Luque-Caballero,¹ Alberto Martín-Molina,¹ and Manuel Quesada-Pérez^{2, a)}

¹Grupo de Física de Fluidos y Biocoloides, Departamento de Física Aplicada, Facultad de Ciencias, Universidad de Granada, 18071 Granada, Spain

²Departamento de Física, Escuela Politécnica Superior de Linares, Universidad de Jaén, 23700 Linares, Jaén, Spain

(Received 6 March 2014; accepted 11 April 2014; published online 1 May 2014)

Both experiments and theory have evidenced that multivalent cations can mediate the interaction between negatively charged polyelectrolytes and like-charged objects, such as anionic lipoplexes (DNA-cation-anionic liposome complexes). In this paper, we use Monte Carlo simulations to study the electrostatic interaction responsible for the trivalent-counterion-mediated adsorption of polyelectrolytes onto a like-charged planar surface. The evaluation of the Helmholtz free energy allows us to characterize both the magnitude and the range of the interaction as a function of the polyelectrolyte charge, surface charge density, [3:1] electrolyte concentration, and cation size. Both polyelectrolyte and surface charge favor the adsorption. It should be stressed, however, that the adsorption will be negligible if the surface charge density does not exceed a threshold value. The effect of the [3:1] electrolyte concentration has also been analyzed. In certain range of concentrations, the counterion-mediated attraction seems to be independent of this parameter, whereas very high concentrations of salt weaken the adsorption. If the trivalent cation diameter is doubled the adsorption moderates due to the excluded volume effects. The analysis of the integrated charge density and ionic distributions suggests that a delicate balance between charge inversion and screening effects governs the polyelectrolyte adsorption onto like-charged surfaces mediated by trivalent cations.

© 2014 AIP Publishing LLC. [<http://dx.doi.org/10.1063/1.4872263>]

I. INTRODUCTION

The interaction between polyelectrolytes (PEs) and charged surfaces has been the subject of many investigations during the last four decades due to their use in industrial applications and in biological processes.^{1,2} However, there is a renewed interest in this problem at present due to its importance in the formation of PE multilayers and in the complexation of PEs with charged particles.³⁻⁶ In particular, the adsorption of PEs on *oppositely* charged substrates of different geometries has been the subject of numerous experimental, theoretical, and simulation studies.⁵⁻¹⁸ From a simplistic electrostatic analysis, it could be concluded that PE adsorption onto an oppositely charged surface should be a spontaneous process electrostatically driven. However, it is a complex issue which has been found dependent on a broad range of facets.⁶ Consequently, PE adsorption onto oppositely charged substrates has been analyzed as a function of: charge, chain stiffness and length of the PE, surface charge density and charge distribution of the substrate, solvent quality for the PE backbone, strength of the short-range interactions between PEs and substrates, conformational transformations in adsorbed PEs, pH and salt concentrations in the media, etc. . . .⁵⁻¹⁸ In contrast, the adsorption of PEs onto like-charged surfaces is a more recent theme that has been scarcely studied. The ability to

control the interaction of PEs, such as DNA or proteins, with similarly charged surfaces has recently attracted a growing interest due to its importance for a multitude of biotechnological applications. For instance, the adhesion and desorption of DNA onto solid surfaces can be controlled by tuning the charge of the surface.¹⁹ In these experiments, large adhesion forces are obtained in the case of a positive electrode, and the adhesive force over DNA is completely suppressed by tuning the charge of the electrode to negative. Also, there is a lot of interest in the possibility of binding DNA to negatively charged liposomes for gene therapy applications (anionic lipids are preferred over cationic ones due to biocompatibility issues).²⁰

Messina *et al.*, were pioneers in the field of the complexation between a negatively charged sphere and a long flexible anionic PE in the presence of multivalent counterions but in a salt-free environment.^{21,22} These authors considered different coupling regimes as well as the influence of the linear charge density (λ) of the PE chain by using Molecular Dynamics (MD) simulations within the framework of a coarse-grained (CG) model. To this end, they used the original definition of the *electrostatic coupling parameter* (Ξ) which uniquely describes different physical regimes that may be found for counterions of charge q at a planar charged wall with a surface charge density σ .²³ This parameter can be calculated as $\Xi = 2\pi q^3 l_B \sigma$, where l_B is the Bjerrum length which measures the distance at which the electrostatic energy of two elementary charge equals the thermal energy $k_B T$. Under a strong

^{a)} Author to whom correspondence should be addressed. Electronic mail: mquesada@ujaen.es

Coulomb coupling regime ($\Xi \gg 1$), structural ion correlations can lead to dominant attractive forces of mainly energetic origin between like-charged surfaces.²⁴ According to the findings obtained by Messina *et al.*, two important conclusions arise: on the one hand, the PE chain is always adsorbed as a flat structure under strong Coulomb coupling regime, and its conformation strongly depends on λ . On the other hand, upon reducing λ the chain tends to spread more and more over the particle surface. Under aqueous conditions, complexation can be obtained with multivalent counterions for high enough values of λ , where the formation of loops was reported.^{11,21,22} Jimenez-Ángeles *et al.* considered a simple model to study the attraction between two like-charged parallel rods immersed in an electrolyte solution.²⁵ Later, Wang *et al.*, used a nonlocal density functional theory (NLDFT) to conclude that the PE adsorption onto a like-charged plane requires the presence of salt containing multivalent counterions being such attraction little influenced by the PE chain length.²⁶ More recently, Turesson *et al.* used also a CG model to perform Monte Carlo (MC) simulations to investigate the calcium mediated PE adsorption onto a like-charged surface.²⁷ Therein the authors concluded that a purely electrostatic adsorption is achieved but can be considerably increased if ion pairing effects between calcium and carboxylate monomers are taken into account. Similar MC simulations, but using a model with inhomogeneous surfaces containing positive and negative charges, were considered by Dias *et al.*^{12,16} These authors also evidenced the adsorption of anionic PEs on a neutral and even a weakly negatively charged surface (overall negative charge but containing both positive and negative surface charges). Unlike the case of a homogeneously charged surface, no addition of multivalent ions was required to obtain PE adsorption onto a like-charged surface. This attraction requires a high flexibility of the PE (in order to adapt to the charge patterns of the surface) and the adsorption reported is significant only for mobile surface charges, since in this case surface charges can create attractive patches for electrostatic adsorption of PEs.^{12,16}

Concerning the adsorption of DNA onto like-charged lipid surfaces mediated by multivalent cations, Liang *et al.* investigated experimentally the complexation of DNA with diverse mixtures of zwitterionic and anionic liposomes in the presence of different divalent metal cations.²⁸ These authors proved that the type and concentration of lipids and cations are determinant in the resulting complex. More recently, it has also been experimentally demonstrated, by analyzing the interaction of linear DNA with anionic lipid monolayers mediated by Ca^{2+} , that the conformation of the resulting complex depends on the surface pressure.²⁹ Although the specific mechanisms involved in the interaction between DNA and like-charged substrates still remain unclear, very recent all-atomic MD simulations have proved that hydrogen bonding can be the dominant force at short distances.^{4,20} Furthermore, short-range specific interactions (solvent mediated, hydrogen bonding) and electrostatic correlations are not independent phenomena in the adsorption of PEs onto like-charged surfaces. Rather, they are correlated and one effect reinforces the other.^{4,20} Unfortunately, specific interactions are not always straightforwardly considered within the theoretical models

and the interaction potential is frequently written into different and additive contributions of the different forces. For instance, in the MC simulations performed by Turesson *et al.*, a specific interaction between a monomer of the PE and a Ca^{2+} ion is modeled by a nonelectrostatic potential (see Eq. (2) in Ref. 27). As a result, they observed that the adsorption behavior was modulated by the electrostatic interactions, while the ion-pairing ones enhanced the adsorption onto the like-charged surface. In line with these authors, a similar type of nonelectrostatic potential is considered by Jorge *et al.*, in their study of DNA-polyethylenimine (PEI)- Fe^{3+} complexes by using MC simulations as well.³⁰ Therein, this interaction energy is justified in terms of the specific chelation of Fe^{3+} by the PEI.

In general, the research works described above promote the idea that correlations of electrostatic origin can provide an attractive (short range) force, strong enough to retain PE adsorbed at like charged surfaces. These correlations can be generated by addition of multivalent ions or by using a responsive surface. Accordingly, the goal of the present work is to find out the conditions at which a purely electrostatic adsorption of PEs onto like-charged planar surfaces can take place. To this end we will focus on the analysis of the free energy of a single chain of PE as a function of its distance from the surface, which becomes an innovative approach itself. The few previous works that have simulated the adsorption of PEs onto like-charged objects characterized this phenomenon through the quantity of polymer in the immediate vicinity of the charged object.^{26,27} In this work, however, the computation of the free energy provides additional (and novel) information on the strength of the attraction between the chain and the surface as well as its range. We will also try to correlate the features of this interaction with underlying mechanisms, such as charge inversion. Given that this information about the effective surface-PE interaction is absent in preceding surveys, the effect of properties such as the charge of the PE and substrate and salt concentration is systematically examined. We have also analyzed the effect of ionic size, which is often omitted. Accordingly, MC simulations were performed within a CG model in conditions in which strong ionic correlations are expected, i.e., highly charged PEs and substrates, in the presence of moderately high concentration of trivalent salt.

The paper is organized into different sections. In Sec. I, the method followed in the MC simulations is described in detail. Later, the effects of the number of charged groups per PE, the surface charge density of the substrate, the electrolyte concentration, and the ionic size are examined. Finally, some conclusions are highlighted.

II. MODEL AND SIMULATIONS

A. Model

Simulations have been performed using a CG model whose main features are: (i) PE chains were modeled by a bead-spring polymer model that has been described elsewhere in the literature;^{10,12} (ii) ions are explicitly considered; (iii) the charged surface is assumed to be planar; (iv) the solvent (water) is taken into account only through its dielectric

permittivity (primitive model). Similar models have been employed by other authors.^{12,16,27}

The negatively charged PE chain is described as a sequence of certain number of hard spheres (beads), N_{bead} , connected with harmonic bonds. In this work $N_{bead} = 20$. The number of charged beads per chain is f . The charge of the beads remains fixed (it is not transferred from one bead to another). It should be kept in mind, however, that the adsorption of a single PE chain onto a planar surface has been simulated in this work, as some authors have previously done.^{12,16} It should be mentioned, however, that other authors have performed studies in which PE chains adsorb from a solution.^{26,27} Although these two kinds of surveys may lead to similar conclusions, the explored situations, the employed techniques, and the examined properties are not the same.

The simulation cell also contains trivalent cations and monovalent anions (in a fixed number given by the bulk electrolyte concentration) as well as the excess of trivalent cations required to have an electroneutral system. All of them are treated as hard spheres. The simulations of this work have been performed assuming that the surface charge is uniformly smeared out. An impenetrable charged wall is located at $z = 0$, whereas at $z = L$ another impenetrable wall without charge is placed.

B. Interactions

The short-range repulsion between any pair of particles (beads and ions) due to excluded volume effects is modeled by means of the usual potential for hard spheres (u_{HS}):

$$u_{HS}(r) = \begin{cases} \infty & r \leq (d_i + d_j)/2 \\ 0 & r > (d_i + d_j)/2 \end{cases}, \quad (1)$$

where r is the center-to-center distance between a given pair of particles and d_i is the diameter of species i . The diameter of all the particles is $d_m = 0.4$ nm although a value of $d_i = 0.8$ nm was also used for ions. The beads of a given chain are connected by harmonic bonds, whose interaction potential is

$$u_{bond}(r) = \frac{k_{bond}}{2}(r - r_0)^2, \quad (2)$$

where k_{bond} is the elastic constant and r_0 is the equilibrium bond length. In this work, we have assumed that $r_0 = 0.5$ nm and $k_{bond} = 0.4$ N/m. This k_{bond} -value has been widely used for polymer chain and networks.³¹⁻³⁴ All the charged species (charged monomers and ions) interact electrostatically through the Coulomb potential:

$$u_{elec}(r) = \frac{Z_i Z_j e^2}{4\pi\epsilon_0\epsilon_r r}, \quad (3)$$

where Z_i is the valence of species i , e is the elementary charge, and $\epsilon_0\epsilon_r$ is the permittivity of the solvent. The interaction energy of ion i with the uniformly charged surface is

$$u(\vec{r}_i) = -\frac{\sigma_0 Z_i e z_i}{2\epsilon_0\epsilon_r}, \quad (4)$$

where \vec{r}_i is the position vector of particle i , z_i is its z -coordinate, and σ_0 is the surface charge density of the charged wall.

At this point, it should be mentioned that we have assumed the walls located at $z = 0$ and $z = L$ have the same dielectric constant as the solvent. This assumption, also made by other authors, allows us to discard image charge effects associated to dielectric discontinuities. In the last decade, several authors have analyzed the influence of image charges on the EDL and PE adsorption under different conditions (see, for instance, the works by Wang *et al.* and Seijo *et al.* and the references cited therein).^{35,36} In any case, these effects are highly specific. For instance, they are expected to be different for a liposome, which involves two dielectric discontinuities and encapsulates an aqueous medium, and a solid substrate. Since we are rather interested in non-specific systems and general trends, image charge effects go beyond the scope of this work.

C. Simulation details

The simulations were carried out in a canonical ensemble employing the standard Metropolis algorithm. Particles were confined in a rectangular prism of dimensions $W \times W \times L$, which must be carefully chosen: both L and W must be much larger than the Debye length of the system, that is, the distance beyond electrostatic interactions is significantly screened. The Debye length is given by $l_D = 1/\sqrt{8\pi l_B I N_A}$, where N_A is the Avogadro number and I is the ionic strength. In addition, W was chosen to be of the order of L , as other authors have done.^{37,38} Before performing simulations in the presence of the PE chain, it is advisable to check, particularly at high charge densities, that cationic and anionic profiles reach well defined and stable values far from the charged surface and do not exhibit noticeable and little reliable border effects near the neutral wall.

Periodic boundary conditions were used in the lateral directions (x and y). The long-range electrostatic interactions were handled using a classical method for the slab geometry put forward by Torrie and Valleau in the early 80s, which we will refer to as the *external potential method* (EPM).³⁷ Each charged particle is allowed to interact with the others in the simulation cell according to the usual minimum image convention. The interaction with the charges outside the cell is considered through an external potential, $\psi_{ext}(z)$, which is calculated assuming that the ionic distribution profiles outside the cell are identical to those inside. In a previous work, the ionic profiles and electrostatic potentials obtained from EPM in the presence of divalent and trivalent counterions were compared to those obtained from the so-called Lekner-Sperb method.³⁹ In general, the agreement was quite good, which supports its reliability. In addition, simulations performed within this approximation were able to capture the behavior of electrophoretic mobility data of latex particles in the presence of divalent and multivalent counterions.⁴⁰ What is more, the existence of charge inversion was proved using a simple model in which only electrostatic interactions between ions and charged surface were considered.⁴⁰ We should also

mention that there is a more refined method (inspired in the EPM) but also more time-consuming.⁴¹

All the particles execute translational moves and, following the recommendations of other authors,^{31,42,43} two additional types of moves were tried in the case of PE chain: (i) translation of the entire chain; (ii) slithering, where one of the end beads is moved to the opposite end of the chain. The translation of the entire chain is advisable because the movement of its center of mass might become extremely slow. Single particle moves were attempted 100 times more often than the other two types of moves. The acceptance ratio, which is the ratio between the accepted moves and the total number of moves in a simulation, was kept between 0.3 and 0.7, according to the rule-of-thumb for obtaining reasonable statistics. It should be also mentioned that maximum displacements permitted in trail moves for chain beads and ions must be different so that the acceptance ratio of each of these particles satisfies this rule-of-thumb. The systems were always equilibrated (at least during 2×10^6 moves) before collecting data for averaging. Our code was checked computing the number of adsorbed monomers onto an oppositely charged surface of $+0.02 \text{ C/m}^2$ (in the presence of monovalent counterions). Dias *et al.* reported results for this case.¹² Although they considered discrete surface charges, good agreement was found (as expected if the surface charge density is large enough).

D. Free energy calculations

In this work the strength of the attraction between the surface and the polymer will be characterized through the Helmholtz free energy of the system formed by the surface, the PE chain, and the electrolyte solution. In our case, we will examine different positions of the center of mass (CM) of the PE chain averaging on statistically representative configurations of the chain and the ionic cloud.

The free energy when the CM of the PE chain is located at a distance z from the charged surface can be computed as^{44,45}

$$F(z) = -k_B T \ln(P(z)) + F_0, \quad (5)$$

where $P(z)$ is the probability density to find the CM of the PE at a distance z and F_0 is an undetermined constant. Here, F_0 will be adjusted so that $F(z)$ tends to 0 far from the surface. According to Eq. (5), the straightforward determination of $F(z)$ requires to compute the number of times that different positions of the CM are visited during a MC trajectory. The histogram obtained from this analysis is proportional to $P(z)$ and its logarithm determines $F(z)$. In practice, however, we can find some problems. For instance, the movement of the CM of long PE chains might become extremely slow. Consequently, the displacement along the whole cell would require a prohibitive number of moves. In addition, some configurations could be rarely visited and relatively poor statistics will be acquired for them. Umbrella sampling methods help to avoid these difficulties.^{44,45} It consists in the introduction of a bias potential that favors configurations that are rarely visited. A particular and simple choice for this case is the window

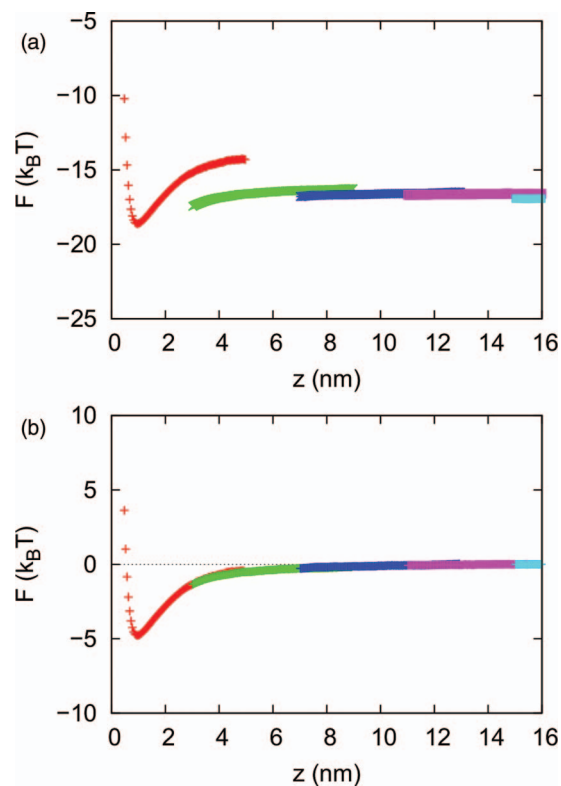


FIG. 1. Helmholtz free energy (F) as a function of the distance of the center of mass of the PE to the charged surface (z) in each window for the case $\sigma_0 = -0.20 \text{ C/m}^2$, an electrolyte concentration of 30 mM, and a PE chain with 5 elementary charges. (a) Raw data. (b) Continuous curve obtained assuming that the adjacent windows have points in common.

potential:

$$W(z) = \begin{cases} 0 & z_{\min} < z < z_{\max} \\ \infty & \text{otherwise} \end{cases}, \quad (6)$$

where z_{\min} and z_{\max} are the lower and upper limits of the window, respectively. Note that this potential restricts the movement of the chain CM between z_{\min} and z_{\max} but the beads of the chain can individually visit the region out of these limits. The cell can be divided into certain number of windows like this one (in the z -direction). For each of these windows, a histogram is obtained. Figure 1(a) shows an example of the free energy obtained in each window for the case $\sigma_0 = -0.20 \text{ C/m}^2$, an electrolyte concentration of 30 mM, and a PE chain with 5 elementary charges. As can be seen, this curve is not continuous. The reader should note that the free energy is determined in each window to within an additive constant, which is related to the normalization constant of the probability density in each window. After exploring the whole cell in this way, the complete free energy can be reconstructed recalling that this function must be continuous from one window to the next. This is equivalent to adjusting the additive constant from one window to the next. Figure 1(b) shows the continuous curve obtained assuming that the adjacent windows have points in common. As can be seen, we have used overlapping windows, which facilitates the connection of the functions belonging to adjacent windows.

III. RESULTS

A. Influence of the polyelectrolyte charge

First we will analyze how the Helmholtz free energy changes with the PE charge. In Figure 2(a), we show $F(z)$ (denoted as F for simplicity) for different numbers of charged monomers in the chain (f). In particular, simulations for $f = 5, 10,$ and 20 were performed with a surface charge density of -0.20 Cm^{-2} , in the presence of 30 mM MX_3 ([3:1] salt). As can be seen, the Helmholtz free energy profiles increase asymptotically at very short distances to the charged plane, display a minimum (denoted as F_{min}) at a short distance ($z = 0.88 \pm 0.16 \text{ nm}$), and converge to 0 at high distances. Therefore, at very short distances, volume excluded effects dominate the interaction producing a strong repulsion. When the PE separates to avoid contact with the plane at short distance, favorable electrostatic interactions between the PE and the adsorbed trivalent cations attract the PE and promote the adsorption. However, if the distance from the PE to the charged plane keeps increasing, then electrostatic interactions are screened and the charged surface does not influence the PE anymore. Therefore, if the adsorbed PE moves beyond the minimum region, then it does not immediately *readsorb* because there is no direct attractive force driving it to the well of the potential. Thus, these curves provide valuable informa-

tion about the strength and range of the electrostatic attractive interaction between the surface and the PE.

More specifically, Figure 2(a) reveals that the PE charge (f) has a clear effect on the strength of this attractive interaction: the more charged the PE is, the deeper the F well is. This dependence can be clearly illustrated plotting the absolute value of F_{min} ($|F_{min}|$) as a function of f (see the inset of Figure 2(a)). The uncertainty estimated for F_{min} from three different simulations would not exceed $1 k_B T$. In agreement with the results shown in Figure 2(a), Messina *et al.* observed that M^{3+} -mediated PE adsorption onto a like-charged sphere was favored by the total PE charge and a poorly charged PE was strongly repelled from the particle in aqueous solution.²¹ Additionally, Turesson *et al.* simulations with increasing polymerization degree PEs produced an increase in the surface excess of PE monomers, what confirms that the Ca^{2+} -mediated PE adsorption is enhanced by the total PE charge.²⁷ In conclusion, total PE charge modulates the adsorption onto a like-charge surface.

We have also obtained additional information about the intensity of the adsorption from the number of mean adsorbed monomers (N_{ad}) and its standard deviation (s), which were computed adopting as criterion that a monomer is adsorbed when its distance to the charged surface is equal or less than 1 nm . In addition, simulations where the CM of the PE is restricted to the interval between $z = 0$ and $z = 5 \text{ nm}$ were employed because the F minimum is located in this interval in all the cases. The results for $f = 5, 10,$ and 20 are $N_{ad} = 8 \pm 4, 11 \pm 3,$ and 12 ± 3 , respectively. Again there is a direct correlation between the number of adsorbed monomers and the PE charge. Accordingly, Dias *et al.* observed $N_{ad} = 20$ in a simulation for a 50-monomer PE interacting with a negatively charged responsive surface,³¹ being the mean adsorbed monomers-total PE monomers ratio similar to the results reported here.

To give insight into the PE adsorption onto like-charged surfaces, it is quite instructive to analyze the ionic profiles in the simulation cell in the absence of PE. For that reason, ion distribution functions ($g(z)$) for counterions (M^{3+}) and coions (X^-) as well as the charge density profile are shown in Figure 2(b) (inset). M^{3+} adsorption onto the negatively charged surface is evident from its distribution function $g_M(z)$ which increases several orders of magnitude over the value in bulk at short distances from the charged plane. In addition, the presence of a maximum in the coion profile ($g_X(z)$) together with a minimum in $g_M(z)$ at $z = 1.2 \text{ nm}$ reveals that there is a considerable accumulation of coions near the adsorbed counterions. Quesada-Pérez *et al.* also reported this kind of electric double layer at similar conditions by both hypernetted-chain/mean-spherical-approximation (HNC/MSA) theory and MC simulations.³⁹ This characteristic electrolyte organization also suggests that the electric double layer has undergone the phenomenon known as charge inversion in the region near the negatively charged surface. This effect can be more clearly appreciated plotting the integrated surface charge density, $\sigma_{int}(z)$ (see Figure 2(b)), which is calculated integrating the contributions from the negatively charged surface and all the particles enclosed between the charged surface and a parallel

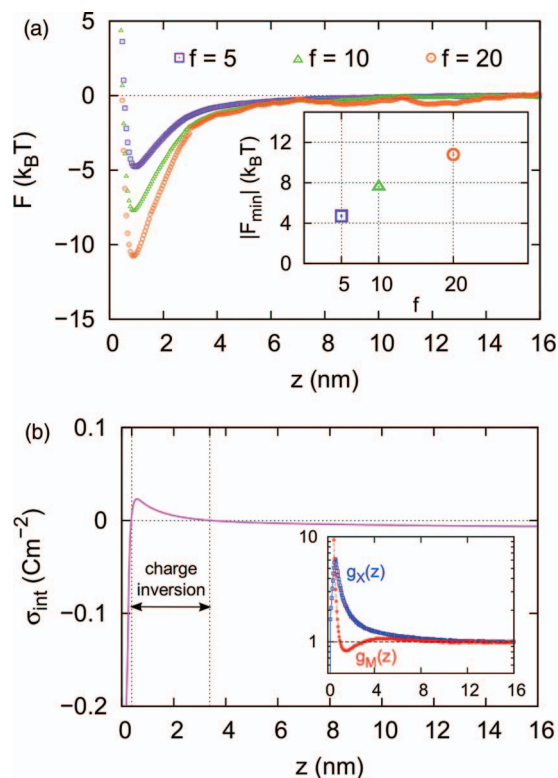


FIG. 2. (a) Helmholtz free energy (F) as a function of the distance of the center of mass of the PE to the charged surface (z), for 20-monomer PEs with different number of charged monomers $f = 5$ (squares, purple), $f = 10$ (triangles, green), $f = 20$ (circles, orange). The monomer charge is $-e$. The surface charge density is -0.20 Cm^{-2} and the MX_3 concentration is 30 mM . Inset: Absolute value of the minimum of F ($|F_{min}|$) as a function of f . (b) Integrated charge density σ_{int} as a function of z for $f = 20$. Inset: Counterion and coion distribution functions, $g_M(z)$ (red) and $g_X(z)$ (blue), respectively, for $f = 20$.

plane placed at a distance z . As can be seen, $\sigma_{int}(z)$ is negative at the immediate vicinity of the negatively charged plane but becomes positive where the charge inversion takes place, in the region between $z = 0.4$ and 3.4 nm, approximately. At higher distances, $\sigma_{int}(z)$ converges to zero, indicating the neutralization of the surface charge in the bulk. Similar profiles of $\sigma_{int}(z)$ were obtained by Wang *et al.* by using the NLDFT model in the presence of PE.²⁶ Additionally, Turesson *et al.* reproduced this charge inversion profile with MC simulations for linear and branched negatively charged polymers interacting with like-charged surfaces in the presence of Ca^{2+} .²⁷ Importantly, the charge inversion region marked in Figure 2(b) reasonably matches the previously mentioned F_{min} region. This fact in conjunction with the M^{3+} adsorption onto the negatively charged surface evidenced by $g_M(z)$ validates the hypothesis formulated above about the essential role of the M^{3+} in the PE adsorption onto a like-charged surface, by creating favorable electrostatic interactions.

B. Influence of the surface charge density

In this section, we explore the role of the surface charge density in the PE adsorption onto like-charge surfaces. To this aim, we performed simulations at the charge densities $\sigma_0 = -0.04$, -0.12 , and -0.20 Cm^{-2} , whereas other parameters were kept constant. In Figure 3(a) we show the results for the system Helmholtz free energy F as a function of the distance of the PE to the charged plane z , for the three different surface charge densities studied. As can be seen, $|F_{min}|$ increases when the surface is more negatively charged (see Figure 3(a), inset). Accordingly, the most intense adsorption would take place at the charge density of $\sigma_0 = -0.20 \text{ Cm}^{-2}$. On the contrary, the adsorption would be negligible at $\sigma_0 = -0.04 \text{ Cm}^{-2}$. To confirm these expectations, we have also quantified the magnitude of the adsorption with the number of mean adsorbed monomers ($N_{ad} \pm s$), being 4 ± 4 , 9 ± 4 , and 12 ± 3 for $\sigma_0 = -0.04$, -0.12 , and -0.20 Cm^{-2} , respectively. The tendency of these values is the same as $|F_{min}|$ (Figure 3(a), inset) and, since $N_{ad} = s$ for $\sigma_0 = -0.04 \text{ Cm}^{-2}$, there is no clear evidence of adsorption at this surface charge density.

In agreement with the results shown in Figure 3(a), Wang *et al.* observed that M^{3+} -mediated PE adsorption onto like-charged surfaces enhanced when increasing the surface charge density.²⁶ Furthermore, Turesson *et al.* observed an increase in the adsorption excess of PE monomers when they increased the surface charge density in absolute value in the presence of Ca^{2+} .²⁷ On the other hand, Dias *et al.* characterized N_{ad} in simulations with positively charged responsive surfaces and they also found that the more charged the surface was, the more intense the PE adsorption onto oppositely charged surfaces was.³¹

Integrated charge density profiles $\sigma_{int}(z)$ for these systems in the absence of PE are shown in Figure 3(b). The comparison of $\sigma_{int}(z)$ for the three different surface charge densities provides an additional interpretation from the Helmholtz free energy curves shown in Figure 3(a). Charge inversion is evident when σ_0 is -0.20 or -0.12 Cm^{-2} . Moreover,

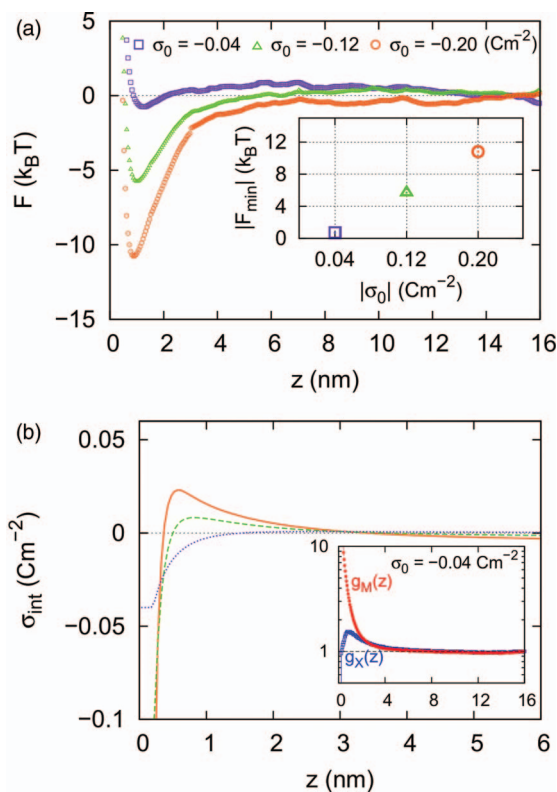


FIG. 3. (a) Helmholtz free energy F as a function of the distance of the center of mass of the PE to the charged surface (z) for PEs interacting with like-charged surfaces of surface charge density $\sigma_0 = -0.04 \text{ Cm}^{-2}$ (squares, purple), $\sigma_0 = -0.12 \text{ Cm}^{-2}$ (triangles, green), $\sigma_0 = -0.20 \text{ Cm}^{-2}$ (circles, orange). All simulations are carried out with a 20 charged monomer PE in the presence of 30 mM MX_3 . Inset: Absolute value of the minimum of F ($|F_{min}|$) as a function of the absolute value of σ_0 . (b) Integrated charge densities σ_{int} as a function of z for $\sigma_0 = -0.04 \text{ Cm}^{-2}$ (dotted, purple), $\sigma_0 = -0.12 \text{ Cm}^{-2}$ (dashed, green), $\sigma_0 = -0.20 \text{ Cm}^{-2}$ (solid, orange). Inset: Counterion and coion distribution functions $g_M(z)$ (red) and $g_X(z)$ (blue), respectively, for $\sigma_0 = -0.04 \text{ Cm}^{-2}$.

$\sigma_{int}(z)$ becomes more positive when $\sigma_0 = -0.20 \text{ Cm}^{-2}$ than $\sigma_0 = -0.12 \text{ Cm}^{-2}$, what means the charge inversion is stronger in the former case. Hence, the attractive surface-PE interaction and the adsorption should be more intense at $\sigma_0 = -0.20 \text{ Cm}^{-2}$ than $\sigma_0 = -0.12 \text{ Cm}^{-2}$, in good agreement with the results shown in Figure 5(a). Importantly, there is no charge inversion at $\sigma_0 = -0.04 \text{ Cm}^{-2}$. Electrophoresis experiments have corroborated this fact.⁴⁶ Accordingly, this feature confirms the role of ionic correlations in promoting the M^{3+} -mediated PE adsorption onto like-charged surfaces via surface charge inversion. Wang *et al.* also observed that the magnitude of this charge inversion increased when the magnitude of the surface charge density, $|\sigma_0|$, was increased.²⁶ However, they used much higher values of $|\sigma_0|$ and they did not explore the lack of charge inversion at low $|\sigma_0|$.

We also represent the counterion and coion distribution functions, $g_M(z)$ and $g_X(z)$, respectively (Figure 3(b), inset) for $\sigma_0 = -0.04 \text{ Cm}^{-2}$. In this case, $g_M(z) \geq g_X(z)$ at all distances from the charged plane z , that is to say, trivalent counterions M^{3+} are adsorbed onto the negatively charged surface, while coions X^- interpenetrate the counterion diffuse layer to compensate the charge. This is in contrast with the ion correlations calculated at $\sigma_0 = -0.20 \text{ Cm}^{-2}$ (Figure 1(b), inset),

where the $g_M(z)$ decreases under $g_X(z)$ and displays a minimum, revealing charge inversion.

C. Radius of gyration

Although this work is not focused on conformational properties, it would be quite instructive to analyze how the conformation of the PE chain changes with the surface charge density (since this parameter has huge influence on adsorption, as discussed previously). The extension of the chain can be characterized by the radius of gyration, but we have preferred to calculate its projections parallel and perpendicular to the charged surface, respectively, defined as¹²

$$\langle R_{G_{xy}}^2 \rangle^{1/2} = \left\langle \frac{1}{N_{bead}} \sum_i [(x_i - x)^2 + (y_i - y)^2] \right\rangle^{1/2}, \quad (7)$$

$$\langle R_{G_z}^2 \rangle^{1/2} = \left\langle \frac{1}{N_{bead}} \sum_i (z_i - z)^2 \right\rangle^{1/2}, \quad (8)$$

where x_i, y_i , and z_i are the Cartesian coordinates of the center of particle i , x, y , and z are the Cartesian coordinates of the CM of the chain, the summation runs over the beads of the chain, and $\langle \dots \rangle$ stands for ensemble average. Figure 4 shows the results obtained for different surface charge densities (and an electrolyte concentration of 30 mM). As can be seen, both projections are considerably smaller than the end-to-end distance that would correspond to a highly extended chain, which means that the PE chain is partly collapsed in the presence of trivalent cations. Our results also show the projection of the radius of gyration onto the xy -plane increases with the absolute value of the surface charge density and the degree of adsorption, whereas the projection in the z -direction decreases. In other words, the chain shrinks in the direction perpendicular to the surface but it expands in the parallel directions. In addition, $\langle R_{G_{xy}}^2 \rangle^{1/2} < \sqrt{2} \langle R_{G_z}^2 \rangle^{1/2}$ for $\sigma_0 = -0.04 \text{ C/m}^2$ but $\langle R_{G_{xy}}^2 \rangle^{1/2} > \sqrt{2} \langle R_{G_z}^2 \rangle^{1/2}$ for $\sigma_0 = -0.20 \text{ C/m}^2$, which implies that the chain is more expanded in the direction perpendicular to the surface for low surface charge density but becomes more expanded in the parallel directions when this parameter grows. In any case, this behavior allows the chain

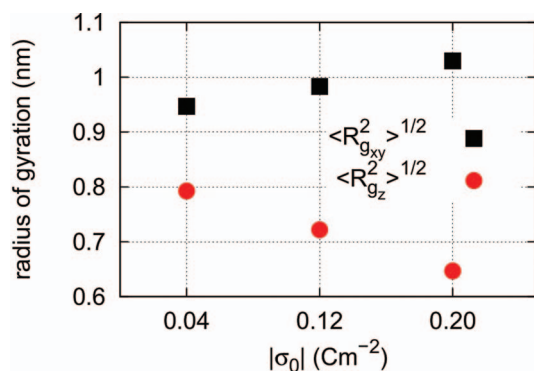


FIG. 4. Projections of the radius of gyration onto the xy -plane (squares) and the z -axis (circles) as a function of the surface charge density. Simulations are carried out with a 20 monomer PE in the presence of 30 mM MX_3 .

to increase the number of beads near the surface and the degree of adsorption when the charge of the surface increases.

D. Influence of the multivalent salt concentration

In this section we analyze how the surface-PE interaction depends on the MX_3 concentration, c . We first present the system Helmholtz free energy F as a function of z for a set of increasing concentrations of MX_3 , $c = 10, 20, 30, 40$, and 90 mM (Figure 5(a)). Although 90 mM is commonly a high concentration for trivalent ions, osmotic stress experiments on DNA in the presence of Co^{3+} solutions up to 100 mM have been performed in the literature.⁴⁷ In addition, high calcium (and sometimes magnesium) concentrations have been also used to mediate polyelectrolyte adsorption on like-charged surfaces in many other systems.²⁷ In any case, we have analyzed this high concentration for theoretical purposes: To find out if the attraction between the PE and the surface displays a non-monotonic behavior with c . The magnitude of $|F_{\min}|$ is plotted as a function of c in Figure 5(a) (inset). As can be seen, the depth of the minimum hardly changes when the concentration is increased from 10 to 40 mM but drops when c is increased to 90 mM. These results for the surface-PE electrostatic interaction (in the presence of trivalent cations) agree with those obtained by Turesson *et al.* for adsorption

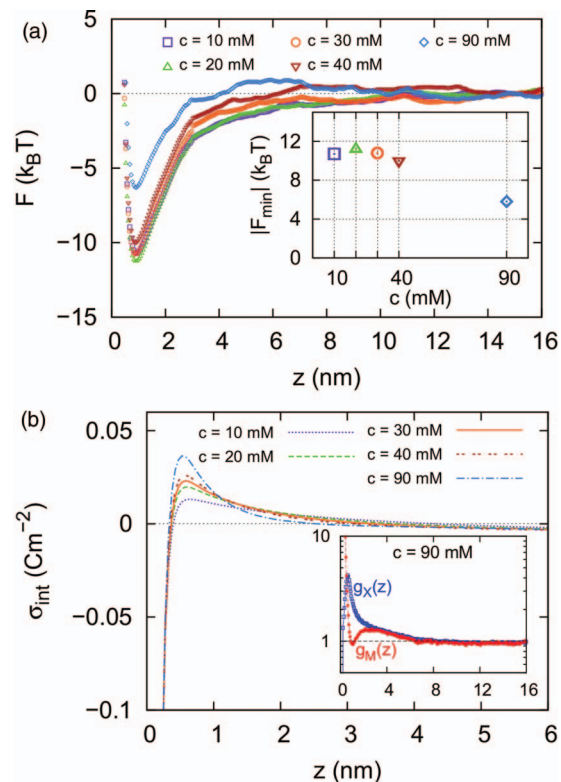


FIG. 5. (a) Helmholtz free energy F as a function of the distance of the center of mass of the PE to the charged surface (z), for a 20 charged monomer PE interacting with a like-charged surface of surface charge density $\sigma_0 = -0.20 \text{ Cm}^{-2}$ in the presence of different MX_3 concentrations: $c = 10 \text{ mM}$ (squares, purple), 20 mM (up triangles, green), 30 mM (circles, orange), 30 mM (down triangles, brown), and 90 mM (inverted squares, blue). Inset: Absolute value of the minimum of F ($|F_{\min}|$) as a function of c . (b) Integrated charge density σ_{int} as a function of z . Inset: Counterion and coion distribution functions, $g_M(z)$ (red) and $g_X(z)$ (blue), respectively, for $c = 90 \text{ mM}$.

onto like-charged surfaces in the presence of Ca^{2+} .²⁷ Ulrich *et al.* also reported a similar behavior for PE adsorption onto an oppositely charged sphere.⁴⁸ It should be also mentioned that Wang *et al.* predicted trivalent-cation-mediated adsorption onto a like-charged planar surface at salt-free solutions and high salt concentrations of the order of 0.5 M, even larger than the values studied in this work, although they did not explore intermediate concentrations.²⁶

Integrated charge distributions represented in Figure 5(b) permit us to elucidate the role of charge inversion in the PE adsorption onto like-charged surfaces at different M^{3+} concentrations. As can be seen, σ_{int} reverses its sign at the charged surface vicinity displaying a maximum that increases with c . Conversely, this c -enhanced charge inversion is not correlated with the PE-adsorption onto the like-charged surface, because at $c = 90$ mM the adsorption diminishes while the magnitude of the charge inversion is the highest. Examining $g_M(z)$ and $g_X(z)$ at this M^{3+} concentration (Figure 5(b), inset), we find that counterions and coions form the electric double layer but, unlike the simulations at $c = 30$ mM (Figure 2(b), inset), the counterions display a pronounced maximum after the minimum. As a consequence, the effect of the charge inversion is totally screened at short distances to the negatively charged plane. In fact, it can be appreciated in the integrated charge distribution at $c = 90$ mM in Figure 5(b), that the charge density drops to zero at shorter distances than the ones at more diluted regimes. In conclusion, the balance between the charge inversion and the screening produced at different MX_3 concentrations determine the magnitude of the PE-adsorption onto like-charged surfaces, being the adsorption optimal at intermediate MX_3 concentrations.

E. Influence of the counterion diameter

Together with electrostatic interactions, volume excluded effects can modulate the surface-PE interaction as well. Furthermore, trivalent cations in solution are covered by a hydration shell that may interfere the direct contact with negatively charged objects. Therefore, simulations with M^{3+} of different diameter allow us to characterize the strength of steric repulsions in the surface/ M^{3+} /PE complex formed upon adsorption.

Helmholtz free energy profiles for PEs interacting with like-charged surfaces in the presence of either 0.4 or 0.8 nm diameter trivalent cations are shown in Figure 6. Both curves display a minimum near the surface. Hence, the PE adsorption onto the like-charge surface takes place when it is mediated by trivalent cations of the studied diameters. However, the adsorption is weaker in the case the M^{3+} diameter $d_M = 0.8$ nm, since its F profile displays a minimum of less absolute value. In other words, doubling the M^{3+} diameter results in a loss of stability in the surface/ M^{3+} /PE complex. Steric repulsion, which is accounted for in these simulations through the hard sphere potential, keeps every pair of particles separated at a distance of at least the sum of their radii. As a consequence, when the M^{3+} diameter is increased, the distance between M^{3+} and the PE monomers and the distance between M^{3+} and the negatively charge plane turns larger and

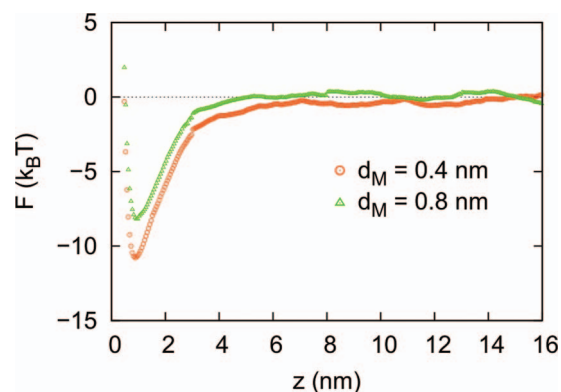


FIG. 6. Helmholtz free energy F as a function of the distance of the center of mass of the PE to the charged surface (z) for a 20 charged monomer PE interacting with a like-charged surface of surface charge density $\sigma_0 = -0.20 \text{ Cm}^{-2}$ in the presence of 30 mM MX_3 for two different trivalent cation diameters: $d_M = 0.4$ nm (circles, orange) and $d_M = 0.8$ nm (triangles, green).

this weakens the electrostatic interactions that stabilize the surface/ M^{3+} /PE complex. In conclusion, the M^{3+} -mediated PE adsorption onto like-charged surfaces is less intense when the M^{3+} diameter is increased.

Remarkably, the results shown in Figure 6 give insight about the role of electrostatic interactions in the PE adsorption onto like-charged surfaces in the presence of hydrated trivalent cations. In this way, the increase in the effective ion radius because of the solvation produces a reduction in the pairwise Coulomb potential between M^{3+} and the negatively charged objects. In fact, the value of $d_M = 0.8$ nm used in this simulation is close to the hydrated ion diameter of some trivalent metals (Al^{3+} - 0.96 nm).⁴⁹ However, the CG model presented here cannot predict the role of water molecules as the solvent is treated as continuum. In this way, all-atomistic simulations could provide valuable information about the effect of the water molecules in the M^{3+} -mediated PE adsorption onto like-charged surfaces, in terms of interaction potential and entropy. The first results in this line with MD simulations have been recently published.^{4,20}

IV. CONCLUSIONS

The trivalent-cation-mediated attraction between a negatively charged surface and an anionic polyelectrolyte chain has been characterized computing the free energy as a function of the distance between them. This method provides information about the strength of such attraction as well as its range, which is limited to a few nanometers in most cases. Beyond this point, these attractive forces would be so weak that they would not lead to adsorption. The effects of the number of charged groups per PE, the surface charge density of the substrate, the electrolyte concentration, and the ionic size have been analyzed in this survey. Our simulations reveal that the intensity of the previously mentioned attraction grows with the charge of the polyelectrolyte chain and the surface. However, this attraction would be negligible if the surface charge density is not high enough. Such a threshold value is the surface charge density required for charge inversion, which confirms that this phenomenon plays

a key role in the adsorption of polyelectrolyte chains onto like-charged substrates. It should be mentioned, however, that the trivalent-cation-mediated attraction can be weakened at high electrolyte concentrations due to electrostatic screening. Our results also prove that small ions favor the polyelectrolyte adsorption.

ACKNOWLEDGMENTS

The authors thank the financial support from the following institutions: (i) “Ministerio de Economía y Competitividad, Plan Nacional de Investigación, Desarrollo e Innovación Tecnológica (I+D+i),” Project Nos. MAT2012-36270-C04-04 and -02. (ii) “Consejería de Innovación, Ciencia y Empresa de la Junta de Andalucía,” Project No. P09-FQM-4698. (iii) European Regional Development Fund (ERDF).

- ¹R. R. Netz and D. Andelman, *Phys. Rep.* **380**, 1 (2003).
- ²A. V. Dobrynin and M. Rubinstein, *Prog. Polym. Sci.* **30**, 1049 (2005).
- ³P. R. Van Tassel, *Curr. Opin. Colloid Interface Sci.* **17**, 106 (2012).
- ⁴J. Faraudo and A. Martín-Molina, *Curr. Opin. Colloid Interface Sci.* **18**, 517 (2013).
- ⁵I. Szilagyí, G. Trefalt, A. Tiraferri, P. Maroni, and M. Borkovec, *Soft Matter* **10**, 2479 (2014).
- ⁶R. Winkler and A. Cherstvy, in *Polyelectrolyte Complexes in the Dispersed and Solid State I*, edited by M. Müller (Springer, Berlin/Heidelberg, 2014), p. 1.
- ⁷H. Boroudjerdi, Y. W. Kim, A. Naji, R. R. Netz, X. Schlagberger, and A. Serr, *Phys. Rep.* **416**, 129 (2005).
- ⁸J.-M. Y. Carrillo and A. V. Dobrynin, *Langmuir* **23**, 2472 (2007).
- ⁹C. F. Nambuena, D. M. Beltramo, and E. P. M. Leiva, *Macromolecules* **40**, 7336 (2007).
- ¹⁰A. V. Dobrynin, *Curr. Opin. Colloid Interface Sci.* **13**, 376 (2008).
- ¹¹R. Messina, *J. Phys.: Condens. Matter* **21**, 113102 (2009).
- ¹²R. S. Dias and A. A. C. C. Pais, *Adv. Colloid Interface Sci.* **158**, 48 (2010).
- ¹³F. Carnal and S. Stoll, *J. Phys. Chem. B* **115**, 12007 (2011).
- ¹⁴A. G. Cherstvy and R. G. Winkler, *Phys. Chem. Chem. Phys.* **13**, 11686 (2011).
- ¹⁵F. Carnal and S. Stoll, *J. Phys. Chem. A* **116**, 6600 (2012).
- ¹⁶R. S. Dias and A. A. C. C. Pais, *J. Phys. Chem. B* **116**, 9246 (2012).
- ¹⁷J. Forsman, *Langmuir* **28**, 5138 (2012).
- ¹⁸F. Xie, T. Nylander, L. Piculell, S. Utsel, L. Wågberg, T. Åkesson, and J. Forsman, *Langmuir* **29**, 12421 (2013).
- ¹⁹M. Erdmann, R. David, A. Fornof, and H. E. Gaub, *Nat. Nano* **5**, 154 (2010).
- ²⁰A. Martín-Molina, G. Luque-Caballero, J. Faraudo, M. Quesada-Pérez, and J. Maldonado-Valderrama, *Adv. Colloid Interface Sci.* **206**, 172 (2014).
- ²¹R. Messina, C. Holm, and K. Kremer, *J. Chem. Phys.* **117**, 2947 (2002).
- ²²R. Messina, C. Holm, and K. Kremer, *Phys. Rev. E* **65**, 041805 (2002).
- ²³R. R. Netz, *Eur. Phys. J. E* **5**, 557 (2001).
- ²⁴A. Naji, M. Kanduč, J. Forsman, and R. Podgornik, *J. Chem. Phys.* **139**, 150901 (2013).
- ²⁵F. Jiménez-Ángeles, G. Odriozola, and M. Lozada-Cassou, *J. Chem. Phys.* **124**, 134902 (2006).
- ²⁶L. Wang, H. Liang, and J. Wu, *J. Chem. Phys.* **133**, 044906 (2010).
- ²⁷M. Turesson, C. Labbez, and A. Nonat, *Langmuir* **27**, 13572 (2011).
- ²⁸H. Liang, D. Harries, and G. C. L. Wong, *Proc. Natl. Acad. Sci. U.S.A.* **102**, 11173 (2005).
- ²⁹G. Luque-Caballero, A. Martín-Molina, A. Y. Sánchez-Treviño, M. A. Rodríguez-Valverde, M. Cabrerizo-Vílchez, and J. Maldonado-Valderrama, *Soft Matter* **10**, 2805 (2014).
- ³⁰A. F. Jorge, R. F. P. Pereira, S. C. C. Nunes, A. J. M. Valente, R. S. Dias, and A. A. C. C. Pais, *Biomacromolecules* **15**, 478 (2014).
- ³¹R. S. Dias, A. A. C. C. Pais, P. Linse, M. G. Miguel, and B. Lindman, *J. Phys. Chem. B* **109**, 11781 (2005).
- ³²M. Quesada-Pérez, J. G. Ibarra-Armenta, and A. Martín-Molina, *J. Chem. Phys.* **135**, 094109 (2011).
- ³³M. Quesada-Pérez and A. Martín-Molina, *Soft Matter* **9**, 7086 (2013).
- ³⁴M. Quesada-Pérez, J. Ramos, J. Forcada, and A. Martín-Molina, *J. Chem. Phys.* **136**, 244903 (2012).
- ³⁵M. Seijo, M. Pohl, S. Ulrich, and S. Stoll, *J. Chem. Phys.* **131**, 174704 (2009).
- ³⁶R. Wang and Z.-G. Wang, *J. Chem. Phys.* **139**, 124702 (2013).
- ³⁷G. M. Torrie and J. P. Valleau, *J. Chem. Phys.* **73**, 5807 (1980).
- ³⁸P. S. Crozier and M. J. Stevens, *J. Chem. Phys.* **118**, 3855 (2003).
- ³⁹M. Quesada-Pérez, A. Martín-Molina, and R. Hidalgo-Álvarez, *J. Chem. Phys.* **121**, 8618 (2004).
- ⁴⁰A. Martín-Molina, J. A. Maroto-Centeno, R. Hidalgo-Álvarez, and M. Quesada-Pérez, *Colloids Surf. A* **319**, 103 (2008).
- ⁴¹D. Boda, K.-Y. Chan, and D. Henderson, *J. Chem. Phys.* **109**, 7362 (1998).
- ⁴²P. Chodanowski and S. Stoll, *J. Chem. Phys.* **111**, 6069 (1999).
- ⁴³P. Chodanowski and S. Stoll, *J. Chem. Phys.* **115**, 4951 (2001).
- ⁴⁴D. Chandler, *Introduction to Modern Statistical Mechanics* (Oxford University Press, 1987).
- ⁴⁵D. Frenkel and B. Smit, *Understanding Molecular Simulation: From Algorithms to Applications* (Academic Press, Inc., 1996).
- ⁴⁶A. Martín-Molina, C. Rodríguez-Beas, R. Hidalgo-Álvarez, and M. Quesada-Pérez, *J. Phys. Chem. B* **113**, 6834 (2009).
- ⁴⁷D. C. Rau and V. A. Parsegian, *Biophys. J.* **61**, 246 (1992).
- ⁴⁸S. Ulrich, A. Laguerre, and S. Stoll, *Macromolecules* **38**, 8939 (2005).
- ⁴⁹J. Israelachvili, *Intermolecular and Surface Forces*, 3rd ed. (Academic Press, 2010).